Solution Structure of a β-Neurotoxin from the New World Scorpion Centruroides sculpturatusEwing

ARTICLE *in* BIOCHEMICAL AND BIOPHYSICAL RESEARCH COMMUNICATIONS · JANUARY 1999

Impact Factor: 2.3 · DOI: 10.1006/bbrc.1998.9904

5 AUTHORS, INCLUDING:

Patricia L Jackson
University of Alabama at Birmingham
65 PUBLICATIONS **1,618** CITATIONS

SEE PROFILE

John O Trent
University of Louisville
131 PUBLICATIONS **5,428** CITATIONS

SEE PROFILE

N Rama Krishna
University of Alabama at Birmingham
126 PUBLICATIONS **3,107** CITATIONS

SEE PROFILE

Biochemical and Biophysical Research Communications **254,** 406–412 (1999)
Article ID bbrc.1998.9904, available online at http://www.idealibrary.com on IDEAL®

Solution Structure of a β-Neurotoxin from the New World Scorpion *Centruroides sculpturatus* Ewing[1]

Michael J. Jablonsky,* Patricia L. Jackson,† John O. Trent,*,‡ Dean D. Watt,§ and N. Rama Krishna*,†,[2]

Comprehensive Cancer Center, †Department of Biochemistry and Molecular Genetics, ‡Division of Hematology and Oncology, University of Alabama at Birmingham, Birmingham, Alabama 35294; and §Department of Biomedical Science, Creighton University, Omaha, Nebraska 68178

Received December 3, 1998

We report the detailed solution structure of the 7.2 kDa protein CsE-I, a β-neurotoxin from the New World scorpion *Centruroides sculpturatus* Ewing. This toxin binds to sodium channels, but unlike the α-neurotoxins, shifts the voltage of activation toward more negative potentials causing the membrane to fire spontaneously. Sequence-specific proton NMR assignments were made using 600 MHz 2D-NMR data. Distance geometry and dynamical simulated annealing refinements were performed using experimental distance and torsion angle constraints from NOESY and pH-COSY data. A family of 40 structures without constraint violations was generated, and an energy-minimized average structure was computed. The backbone conformation of the CsE-I toxin shows similar secondary structural features as the prototypical α-neurotoxin, CsE-v3, and is characterized by a short 2½-turn α-helix and a 3-strand antiparallel β-sheet, both held together by disulfide bridges. The RMSD for the backbone atoms between CsE-I and CsE-v3 is 1.48 Å. Despite this similarity in the overall backbone folding, the these two proteins show some important differences in the primary structure (sequence) and electrostatic potential surfaces. Our studies provide a basis for unravelling the role of these differences in relation to the known differences in the receptor sites on the voltage sensitive sodium channel for the α- and β-neurotoxins.

The venoms from scorpions typically consist of a large number of different proteins responsible for the neurotoxicity of the scorpion sting. Both long chain neurotoxins (MW ~ 7 kDa), which bind to the sodium channels, and short chain toxins (MW ~ 4 kDa), which bind to other channels such as K^+ and Cl^- channels, are typically present in the venom. The long chain scorpion neurotoxins can be usually devided into two classes, α- and β-toxins, on the basis of their effect on the sodium channel (1). The α-toxins slow the inactivation of the sodium ion permeability in the channel. In contrast, the β-toxins shift the voltage of activation toward more negative potentials, causing the membrane to fire spontaneously and repetitively (2). Both toxins make the inactivation of the sodium channel incomplete. Whereas the α-toxins are present in both Old World and New World scorpions, practically all the β-toxins isolated so far are from the New World species (see 2, 3), except for toxins AaH IT4 (which competes weakly with both α- and β-type toxins) and AaH STR1 (an inactive protein which was classified as closely related to β-type toxins from sequence comparison) from the Old World scorpion *Androctonus australis hector* (4, 5). The receptors for these toxins are also different, with the α-toxins binding to site 3 and the β-toxins binding to site 4 on the sodium channel (1,6). All these long-chain neurotoxins are characterized by four disulfide bridges, and highly conserved secondary structural features consisting of a short α-helix and an antiparallel β-sheet (7). In addition, they all have four major loops, J, M, B, and F (2, 8). The relative orientation of the helix and sheet is maintained by a highly conserved structural motif involving two disulfide bridges linking the helix and sheet (9–11). The crystal and NMR structures for several scorpion α-neurotoxins have been reported in literature (e.g., see 5, 7, 8, 11–19). This work presents the first detailed structure of an active β-neurotoxin from scorpion venom.

[1] The coordinates for the $<SA>_k$ family of structures and the energy minimized average structure $<SA>_{kr}$ of CsE-I have been deposited with the Protein Data Bank (Codes 1b3c and 2b3c). The complete proton NMR chemical shifts have been deposited with the BMRB (Accession No. 4279). Support of this work by NSF grant MCB-9630775 and the NCI grant CA-13148 (NMR Facility) is gratefully acknowledged. The authors also thank Dr. Mike Carson of the Center for Macromolecular Crystallography for his assistance with homology modeling of Css-II toxin, and Dr. Ted Sakai for the color prints.

[2] To whom correspondence should be addressed at CHSB-19 B-31, NMR Core Facility, UAB, 933 South 19th Street, Birmingham, AL 35294-2041. Fax: (205) 934-5695. E-mail: nrkrishna@bmg.bhs.uab.edu.

0006-291X/99 $30.00

```
          1         10        20        30        40        50        60
          ↓         ↓         ↓         ↓         ↓         ↓         ↓
CsE-I     KDGYLVEK-TGCKKTCYKLGENDFCNRECKWKHIGGSYGYCYGF--GCYCEGLPDSTQTWPLPNKTC
CsE-v3    KEGYLVKKSDGCKYGCLKLGENEGCDTECKAKNQGGSYGYCYAF--ACWCEGLPESTPTYPLPNKSC
CsE-v1    KEGYLVKKSDGCKYDCFWLGKNEHCNTECKAKNQGGSYGYCYAF--ACWCEGLPESTPTYPLPNKSC
CsE-V     KKDGYPVDSGN-CKYECLK---DDYCNDLCLER--KADKGYCYWGKVSCYCYGLPDNSPTKT--SGKCNPA
Css-II    KEGYLVSKSTGCKYECLKLGDNDYCLRECKQQYGKSSGGYCYAF--ACWCTHLYEQAVVWPLPNKTCN
Cn-1      KDGYLVDA-KGCKKNCYKLGKNDYCNRECRMKHRGGSYGYCYGF--GCYCEGLSDSTPTWPLPNKTCS
```

FIG. 1. Comparison of the amino acid sequences of some α-toxins CsE-v3 (11), v1 (15), V (8) and β-toxins CsE-I (20), Css-II (35), and Cn-1 (3) from the New World scorpions. The C-terminal of CsE-I is found to be amidated based on NMR data.

MATERIALS AND METHODS

The isolation and purification of the CsE-I toxin from CMC Zone 11 from the venom of *C. sculpturatus* by rechromatography has been described elsewhere (2). Its amino acid sequence (Fig. 1) was determined (20) and physiological effects on the sodium current reported (21, 22). The NMR sample consisted of a solution of 1 mM of pure protein dissolved in H_2O with 10% D_2O for deuterium lock, at pH 4. The same sample was lyophilized and redissolved in 99.996% D_2O for additional experiments.

The NMR measurements were performed on a Bruker AM-600 spectrometer equipped with an Aspect 3000 computer. Data were collected at 313 K. 2D NOESY, DQF-COSY and TOCSY measurements were performed in pure absorption mode using time proportional phase increment. Since the amide protons in this protein were found to exchange rather rapidly with the bulk water resulting in substantially diminished intensities for practically all the amide protons on water presaturation, we employed a jump-return read pulse with water flip back for all 2D-NMR measurements in H_2O. Mixing times of 100 ms and 200 ms for NOESY in H_2O, and 200 ms and 400 ms in D_2O were employed. The TOCSY was performed with a mixing time of 65 ms.

The solution structures were generated using a hybrid protocol involving distance geometry (DG) and dynamical simulated annealing (SA) (23, 24) with minor modifications (11) using XPLOR/QUANTA/CHARMM modeling package (Molecular Simulations Inc, San Diego) on an Indigo^2 Workstation (Silicon Graphics Inc). Briefly, distance geometry substructures were first generated using only medium and long range (residues i, i + 2 or greater) distance constraints and torsion angle constraints. Dynamical simulated annealing followed by energy minimization was then performed using a 4-step protocol (11). From among the resulting structures, only those with distance constraint violations less than or equal to 0.3 Å and dihedral angle violations less than or equal to 5 degrees were considered acceptable, designated as $<SA>_k$, and included in the statistical analysis. The average structure $<\overline{SA}>_k$ was computed from the averages of coordinates of atoms. This structure was first subjected to a restrained energy minimization to remove bond angle and bond length distortions and then followed by an unrestrained energy minimization to obtain the final energy minimized average structure $<\overline{SA}>_{kr}$.

DELPHI calculations. The electrostatic potentials were calculated using the nonlinear Poisson–Boltzmann treatment in DELPHI (25) with the AMBER95 (26) charges and van der Waals parameters. The electrostatic potentials were mapped to a molecular surface generated in Grasp (27).

RESULTS

Sequence specific assignments. The sequential assignment of individual residues in CsE-I was made using standard methodology (28) and is based on sequential NOE connectivities of the type αN (i, i + 1), NN(i, i + 1), and βN(i, i + 1). In the case of proline residues, the sequential contacts $\alpha\delta$(i, i +1) and $\beta\delta$(i, i + 1) with the proline δ hydrogens were used to sequentially assign prolines 51 and 60 and establish their trans conformation. Pro58 was assigned from the $\alpha\alpha$(i, i + 1) contact with Trp57, thus also establishing a cis-conformation for this proline. The sidechain protons for each residue were assigned through TOCSY. Stereospecific assignments for the β-methylene protons, and the methyls of valines and leucines were assigned using standard procedures (29).

Experimental constraints. The proton-proton distance constraints in CsE-I were obtained from NOESY cross peak intensities which were grouped as strong (1.8-2.7 Å), medium (1.8-3.3 Å), or weak (1.8-5.0 Å). This classification used the NOESY spectra with mixing times of 100 ms in H_2O and 200 ms in D_2O solutions. The 400 ms NOESY was used only to assign additional long-range contacts. Spin diffusion effects in the 400 ms NOESY effects were carefully screened by considering only those contacts not mediated by intervening protons. A total of 877 NOE constraints were

TABLE 1

Structural Statistics for CsE-I

	$<SA>_k$	$<\overline{SA}>_{kr}$
r.m.s. deviations from experimental distance constraints (Å)		
All (877)	0.00983	0.00500
Sequential ($\|i - j\| = 1$) (228)	0.0129	0.00738
Medium-range ($1 < \|i - j\| < 5$) (66)	0.00769	0.00362
Long-range ($\|i - j\| > 5$) (199)	0.00754	0.00086
Intra-residue (356)	0.00839	0.00494
H-bonds (28)	0.00680	<0.001
r.m.s. deviations from experimental dihedral angle constraints (deg.) (99)	0.178	0.082
Energies (kcal mol^{-1})		
E(nOe)	4.45	1.01
E(tor)	0.326	0.042
E(repel)	5.52	3.49
E(L-J)	−260	−271
Deviations from idealized covalent geometry		
Bonds (Å)	0.00189	0.00158
Angles (deg.)	0.552	0.503
Impropers (deg.)	0.380	0.328

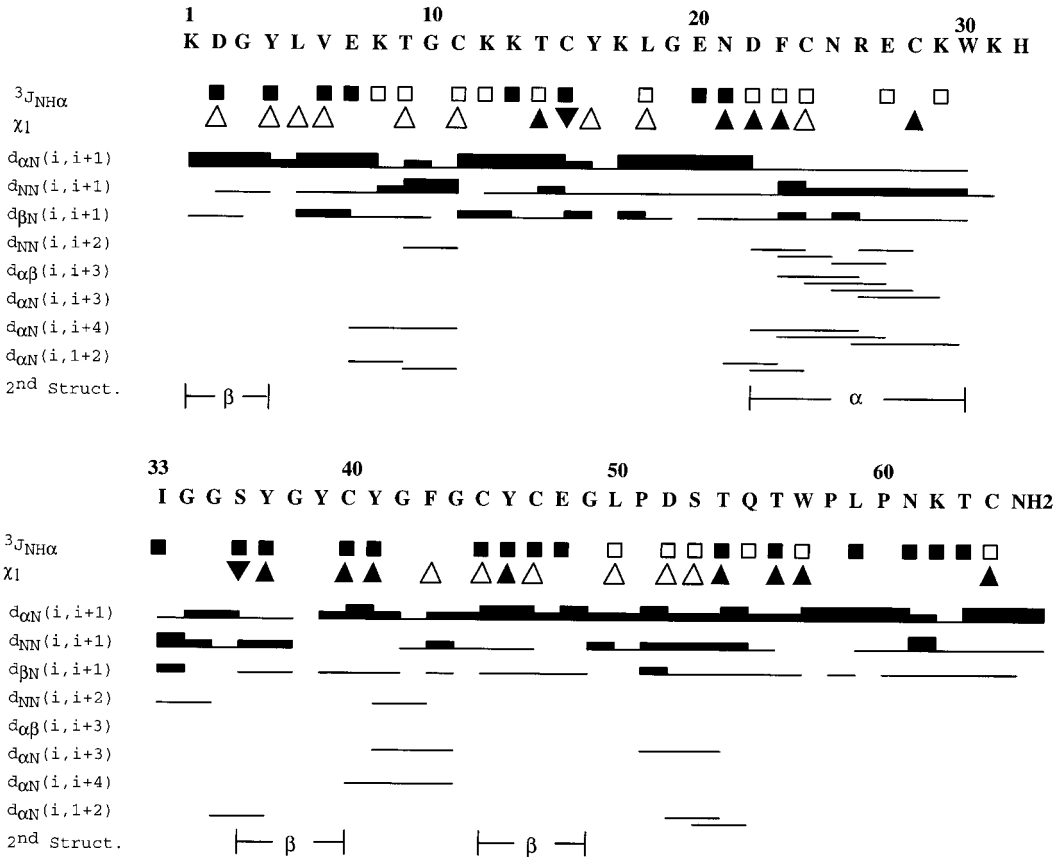

FIG. 2. Summary of NMR data for CsE-I. Sequential NOESY connectivities with amide protons are shown as filled bars, while other connectivities are shown as lines. In the case of prolines, the contacts are to the δ hydrogens. Vicinal coupling constants: $^3J_{N\alpha} > 8$ Hz (■) and $^3J_{N\alpha} < 7$ Hz (□); torsion angles $\chi_1 = 180°$ (▲), 60° (▼), and −60° (△). Regions of α-helix and β -sheet are also shown.

used. Table 1 gives the distribution of NOE contacts identified in this protein in terms of sequential, short range, long range, and intraresidue constraints. Hydrogen bond constraints were included for standard secondary structures. A total of 99 torsion angle constraints were used (40 for ϕ, 29 for ψ, and 30 for χ_1). The constraints of 110° ± 90° for ψ were incorporated when strong αN(i, i + 1) NOE contacts were observed. For $J_{N\alpha} \geq 8$ Hz, ϕ was set to −120° ± 50°; for ≤ 7 Hz, ϕ was set to −65° ± 25°. The χ_1 constraints were determined from stereospecific assignments, and the rotamer angles were restricted to ± 60°. Figure 2 shows a summary of sequential connectivities, together with coupling constant data.

Modeling calculations. Table 2 gives the structural statistics for the CsE-I structures generated using the XPLOR-based DG/SA protocol as described above. A total of 200 structures were generated, of which 40 showed no constraint violations, constituting the $\langle SA \rangle_k$ family. The average structure was computed, and energy minimized to obtain $\langle \overline{SA} \rangle_{kr}$. This structure exhibited an rms deviation of 1.09 Å for the backbone, and 1.71 Å for all atoms, with respect to the family (Table 2). Figure 3 shows 25 typical structures from the family $\langle SA \rangle_k$. A preliminary report of a low resolution structure of this protein from fewer number of constraints has been previously presented (30). Figure 4 shows a superposition of the energy minimized average structure $\langle \overline{SA} \rangle_{kr}$ of the β-neurotoxin CsE-I

TABLE 2

Atomic RMS Deviations (in Å) for the CsE-I and CsE-v3

	Backbone	All atoms
$\langle SA \rangle_k$ vs. $\langle \overline{SA} \rangle_k$	1.10	1.55
$\langle SA \rangle_k$ vs. $\langle \overline{SA} \rangle_{kr}$	1.09	1.71
$\langle \overline{SA} \rangle_k$ vs. $\langle \overline{SA} \rangle_{kr}$	0.40	0.75
$\langle \overline{SA} \rangle_{kr}$ vs. $\langle \overline{SA} \rangle_{dr}$†	0.22	0.28
$\langle \overline{SA} \rangle_{kr}$ vs. CsE-v3 (1-64)	1.48	—
$\langle \overline{SA} \rangle_{kr}$ vs. CsE-v3 (helix and sheet)	0.86	—

† $\langle \overline{SA} \rangle_{dr}$ is the average of the $\langle SA \rangle_k$ structures energy minimized without restraints.

FIG. 3. Best fit superposition of a family of 25 backbone (C_α) structures for CsE-I.

and the crystallographic structure of the very weakly active α-neurotoxin CsE-v3. A model for the prototypical β-toxin Css-II was built by homology modeling using the crystal structure of CsE-v3 (coordinates obtained from Protein Data Bank). The electrostatic potential surfaces for CsE-I, Css-II and CsE-v3 were computed as mentioned before. Figure 5 shows a comparison of the potential surfaces for CsE-I and CsE-v3.

DISCUSSION

Figure 1 shows a comparison of the sequences some of the New World scorpion toxins. CsE-I lacks Ala and Met in its composition. It is also probably the only known long chain scorpion toxin lacking an alanine. The β-toxin CsE-I differs in 20 locations with respect to the α-toxin CsE-v3, which is only weakly toxic. In addition it has an amino acid deletion at position 9 of CsE-v3. When compared to CsE-V, it differs in as many as 28 locations, and also has some significant amino acid insertions and deletions. Like other typical long chain scorpion toxins, CsE-I also is characterized by a 3½ turn α-helix spanning residues 22 to 30, and a short stretch of an antiparallel β-sheet involving residues 1-4, 45-49, and 36-40 (Figure 2). The β-sheet and the α-helix are held together by two disulfide bridges. There is some reasonable degree of similarity of the loop structures (J, M, B, and F) as well. The RMSD between the backbone atoms between the two structures is 1.48 Å (Table 2). Further, as in the case of other scorpion toxins, one side of CsE-I is characterized by a hydrophobic surface rich in aromatic residues, with Y39, Y46 and Y4 in herringbone arrangement. This side is referred to as the front surface. Since chemical modifications of aromatic residues on this conserved hydrophobic surface leads to a loss of activity, this surface has been implicated in binding to the receptor (31, 32). The proteins CsE-v3, v1 and V have some slowly exchanging amide hydrogens with half-life times of several hours at pH 4. In contrast, practically all of the amide protons in CsE-I including those in stable secondary structures have half-life times of less than a minute at pH 4, since on dissolving the protein in D_2O all the amide protons disappear within the first two minutes. This observation suggests that CsE-I adopts a folded but yet highly dynamic (compared to CsE-v3,v1, and V) conformation. It is not clear if this dynamic conformation of CsE-I relates to its activity since another β-toxin isolated from *C. sculpturatus* adopts a rather stable conformation characterized by very slowly exchanging amide hydrogens with half-lifes of several days (unpublished observations).

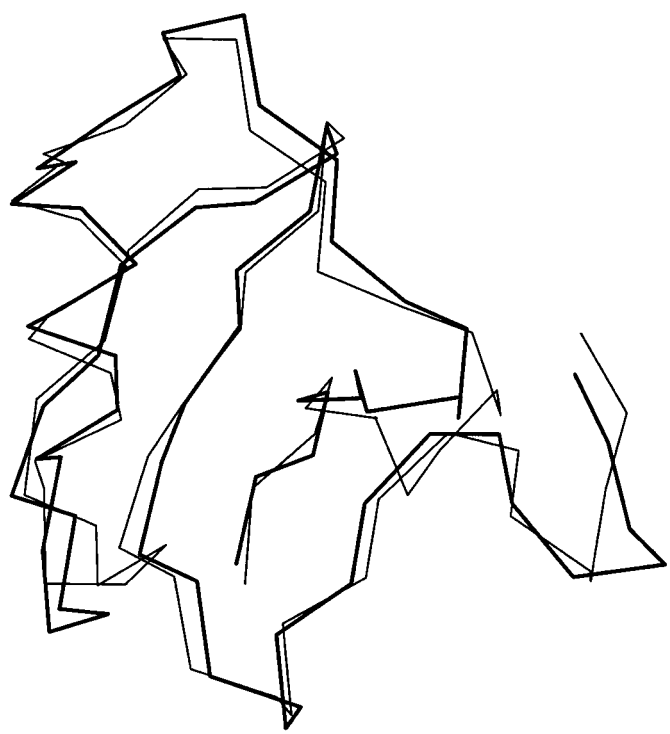

FIG. 4. Best fit superposition of CsE-I (thick line) and CsE-v3 (thin line) backbone structures.

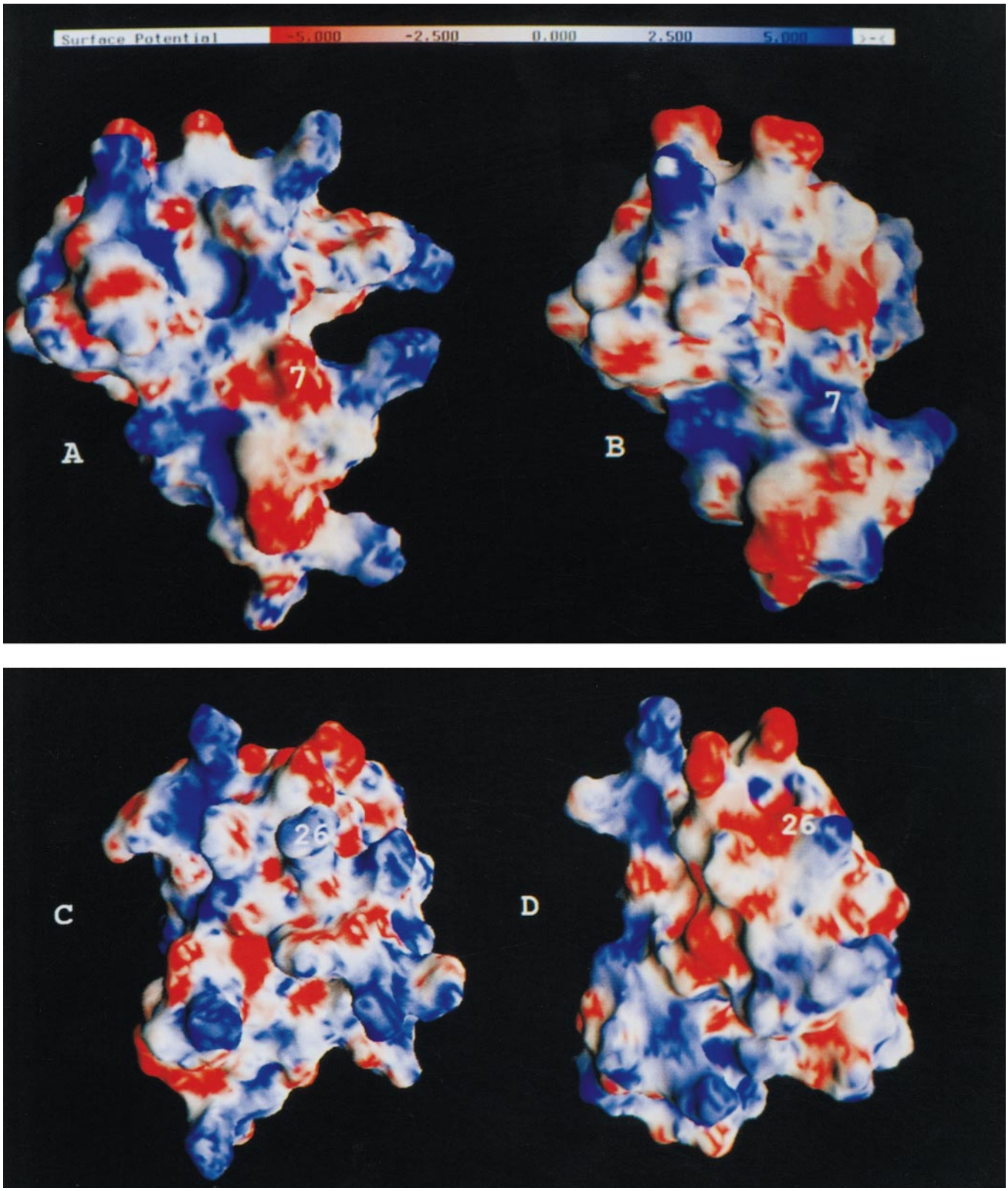

FIG. 5. Electrostatic potential surfaces for CsE-I (left, A, C) and CsE-v3 (right, B, D) showing the differences centered around residue 7 (top, A, B) and residue 26 (bottom, C, D). The potentials are shown at ± 5 kT, with red representing negative and blue positive surfaces.

Despite these apparent similarities in the secondary structures and the general overall folding, there are some important differences at some locations in the sequences of CsE-I and CsE-v3, resulting in significant differences in the hydropathy index and/or electrostatic potential surfaces in the vicinity of these locations. The differences in the sequences are (CsE-v3 to CsE-I): K7 to E7, deletion of S9; D10 to T9, Y14 to K13, G24 to F23; T27 to R26, A31 to W30; N33 to H32; Q34 to I33, P56 to Q55, and S64 to T63. Indeed, some of the differences are reflected in the electrostatic potential surfaces. Figure 5 highlights a couple of differences in CsE-I and CsE-v3 in the vicinity of residues 7 and 26, on the right side of the protein and the top of the helix, respectively. These differences are also preserved between Css-II and CsE-v3 (not shown). In view of the sensitivity of the electrostatic potential surfaces to the orientations of the sidechains, the susceptibility of the surface residue sidechains in crystal structures to packing interactions, and the inherently poor definition of some of these sidechain orientations in solution due to conformational flexibility and lack of constraints, such differences should be approached with some caution. Nevertheless, some of the sequence differences may be significant in light of available chemical modification data on neurotoxins. Such studies on the α-toxin LqhαIT from *Leiurus quinquestriatus hebraeus* indicate that the positively charged residues near the C-terminus may interact directly with the recognition points at the receptor site on the sodium channel (33). Similarly, the modification of residues R60 in AaH-I, R62 in AaH-II, and K-63 in Css-II all result in a loss of pharmacological activity (31). The inversion of charge at position 7 (K7 in CsE-v3 and E7 in CsE-I) may also be significant since a K-to-D mutation at the corresponding location (position 8) in LqhαIT has a profound effect on its biological activity and its electrostatic potential surface (33). The differences in the vicinity of residue 14 (Y14 in CsE-v3 and K13 in CsE-I) may also be important. The probable involvement of Y14 in AaH-III was suggested from chemical modification studies (32). Interestingly, modification of R27 in the β-toxin Css-II, which is in register with R26 in CsE-I and T-27 in CsE-v3, affects antigenic activity but not the pharmacological activity (34). Other significant differences also exist in the potential surfaces between these proteins. Evaluation of the significance of such differences will have to await further chemical modification studies. The observed differences in the sequences and in the electrostatic potential surfaces in this investigation provide a molecular basis for further studies on the interaction of the α- and β-neurotoxins with their receptor sites on the sodium channel.

REFERENCES

1. (a) Gordon, D., Savarin, P., Gurevitz, M., and Zinn-Justin, S. (1998) J. *Toxicol.-Toxin Reviews* **17,** 131–159. (b) Jover, E., Courad, F., Rochat, H. (1980) *Biochem. Biophys. Res. Commun.* **95,** 1607–1614.
2. Simard, J. M., Meves, H., and Watt, D. D. (1992) *in* Natural Toxins: Toxicology, Chemistry and Safety (Keeler, R. F., Mandava, N. B., and Tu, A. T., Eds.), Alaken Inc., pp. 236–263.
3. García, C., Becerril, B., Selisko, B., Delepierre, M., and Possani, L. D. (1997) *Comp. Biochem. Physiol.* **16,** 315–322.
4. Loret, E. P., Martin-Eauclaire, M-F., Mansuelle, P., Sampieri, F., Granier, C., and Rochat, H. (1991) *Biochemistry* **30,** 633–640.
5. Blanc, E., Hassani, O., Meunier, S., Mansuelle, P., Sampieri, F., Rochat, H., and Darbon, H. (1997) *Eur. J. Biochem.* **247,** 1118–1126.
6. Gordon, D., Martin-Eauclaire, M-F., Cestéle, S., Kopeyan, C., Carlier, E., Khalifa, R. B., Pelhate, M., and Rochat, H. (1996) *J. Biol. Chem.* **271,** 8034–8045.
7. Fontecilla-Camps, J. C., Almassy, R. J., Ealick, S. E., Suddath, F. L., Watt, D. D., Feldman, R. J., and Bugg, C. E. (1981) *Trends Biochem. Sci.* **6,** 291–296.
8. Jablonsky, M. J., Watt, D. D., and Krishna, N. R. (1995) *J. Mol. Biol.* **248,** 449–458.
9. Bruix, M., Jimenez, M. A., Santoro, J., Gonzalez, C., Colilla, F. J., Mendez, E., and Rico, M. (1993) *Biochemistry* **32,** 715–724.
10. Bontems, F., Roumestand, C., Boyot, P., Gilquin, B., Doljansky, Y., Menez, A., and Toma, F. (1991) *Eur. J. Biochem.* **196,** 19–28.
11. Lee, W., Moore. C. H., Watt, D. D., and Krishna, N. R. (1994) *Eur. J. Biochem.* **218,** 89–95.
12. Zhao, B., Carson, M., Ealick, S. E., and Bugg, C. E. (1992) *J. Mol. Biol.* **227,** 239–252.
13. Fontecilla-Camps, J. C., Habersetzer-Rochat, C., and Rochat, H. (1988) *Proc. Natl. Acad. Sci. USA* **77,** 6496–6500.
14. Li, H-M., Wang, D-C., Zeng, Z-H., Jin, L., and Hu, R-Q. (1996) *J. Mol. Biol.* **261,** 415–431.
15. Lee, W., Jablonsky, M. J., Watt, D. D., and Krishna, N. R. (1994) *Biochemistry* **33,** 2468–2475.
16. Darbon, H., Weber, C., and Braun, W. (1991) *Biochemistry* **30,** 1836–1845.
17. Landon, C., Sodano, P., Cornet, B., Bonmatin, J. M., Kopeyan, C., Rochat, H., Vovelle, F., and Ptak, M. (1997) *Proteins* **28,** 360–374.
18. Lebreton, F., Ramirez, A. N., Balderas, C., Possani, L.,D., and Delepierre, M. (1994) *Biochemistry* **33,** 11135–11149.
19. Tugarinov, V., Kustanovich, I., Zilberberg, N., Gurevitz, M., and Anglister, J. (1997) *Biochemistry* **36,** 2414–2424.
20. Babin, D. R., Watt, D. D., Goos, S. M., and Mlejnek, R. V. (1975) *Arch. Biochem. Biophys.* **166,** 125–134.
21. Meves, H., Rubly, N., and Watt, D. D. (1982) *Pflugers Arch.* **393,**56–62.
22. Hu, S. L., Meves, H., Rubly, N., and Watt, D. D. (1983) *Pflugers Arch.* **397,** 90–99.
23. Nilges, M., Clore, G. M., and Gronenborn, A. M. (1988) *FEBS Lett.* **229,** 317–324.
24. Driscoll, P. C., Gronenborn,. A. M., Beress, L., and Clore, G., M. (1989) *Biochemistry* **28,** 2188–2198.
25. Gilson, M. K., Sharp, K. A., Honig, B. H. (1988) *J. Comput. Chem.* **9,** 327–335.

26. Cornell, W. D., Cieplak, P., Bayly, C., Gould, I. R., Merz, Jr., K. M., Ferguson, D. M., Spellmeyer, D. C., Fox, T., Caldwell, J. W., Kollman, P. A. (1995) *J. Amer. Chem. Soc.* **117,** 5179–5197.
27. Nicholls, A., Sharp, K. A., and Honig, B. (1991) *Proteins Struct. Funct. Gen.* **11,** 281–296.
28. Wuthrich, K. (1986) NMR of Proteins and Nucleic Acids, Wiley, New York.
29. Basus, V. J. (1989) *Methods Enzymol.* **177,** 132–149.
30. Jackson, P. L., Watt, D. D., and Krishna, N. R. (1994) *Biophys. J.* **66,** A38.
31. Darbon, H. (1990) *in* Protein Structure–Function (Zaidi, Z. H., Abbasi, A., and Smith, D. L., Eds.), pp. 169–181. TWEL Publishers, Karachi.
32. Kharrat, R., Darbon, H., Rochat, H., and Granier, C. (1989) *Eur. J. Biochem.* **181,** 381–390
33. Zilberberg, N., Froy, O., Loret, E., Cestele, S., Arad, D., Gordon, D., and Gurevitz, M. (1997) *J. Biol. Chem.* **272,** 14810–14816.
34. Ayeb, M. E., Darbon, H., Bahraoui, E. M., Vargas, O., and Rochat, H. (1986) *Eur. J. Biochem.* **155,** 289–294.
35. Martin, M. F., Garcia, Y., Perez, L. G., Ayeb, M. E., Kopeyan, C., Bechis, G., Jover, E., and Rochat, H. (1987) *J. Biol. Chem.* **262,** 4452–4459.